Enhancement of Bandwidth-Responsivity Product in High-Speed Avalanche Photodiodes with Optimized Flip-Chip Bonding Package for Coherent Detection

Naseem[1], Nan-Wei Chen[2], Syed Hasan Parvez[1], Zohauddin Ahmad[1], Sean Yang[3], H.-S. Chen[3], Hsiang-Szu Chang[3], Jack Jia-Sheng Huang[3], and Jin-Wei Shi[1*]

[1]*Department of Electrical Engineering, National Central University, Jhongli, Taoyuan, 320, Taiwan*
[2] *Department of Electrical Engineering, Yuan Ze University, Jhongli, 320, Taiwan*
[3]*Source Photonics, No. 46, Park Avenue 2nd Rd., Science-Based Industrial Park, Hsinchu, Taiwan*
**Tel: +886-3-4227151 ext. 34466*
**FAX: +886-3-4255830*
**Email: jwshi@ee.ncu.edu.tw*

Abstract: Flip-chip bonding APDs with 14μm window diameters are demonstrated. Wide-bandwidth (36GHz), high-responsivity (3.4A/W), low dark current (175nA) and high MMW output power (-1dBm at 40GHz) can be achieved simultaneously with 12.5mA I_{sat} under $0.9V_{br}$.

OCIS codes: (040, 1345) Avalanche photodiodes (APDs), (230.5170) Photodiodes

I. Introduction

The bandwidth hungry in modern 5G and cloud communication networks strongly drives the developments of bandwidth capacity for data communication, which migrates from 400 to 800 Gbit/sec. In addition to the intensity modulation and direct detection (IMDD) scheme, coherent communication schemes have become an alternative solution for >100 Gbit/sec data communication [1]. In a coherent receiver-end, the photodiode (PDs) or avalanche photodiodes (APDs) need to sustain high-speed and high-linearity performance under strong (~mW) optical local oscillator (LO) pumping powers to ensure high sensitivity performance [2,3]. As compared to the p-i-n PD counterparts, the APD based receiver has the benefit of higher sensivity (responsivity) with less required optical LO pumping power [3,4]. In order to enhance the saturation power and speed of APDs, both the absorption and multiplication layer thicknesses must be aggressively downscaled, which limits its responsivity performance for wide bandwidth performance (>30 GHz) [5,6] and accompanies with a pronounced leakage current (~1 μA) [5]. Waveguide type APD structure (WGAPD) has been demonstrated to further extend the bandwidth-responsivity product in APD with thin active layers [3,7]. Nevertheless, the alignment tolerance for device package of WGAPD is usually much less than that of the vertical-illuminated counterpart and the significant insertion loss of passive optical components on photonic integrated circuits (PICs) platform for monolithic integration with WGAPD remains a challenge [3,7]. Backside-illuminated structure with flip-chip bonding package is an alternative solution to relax the low-responsivity problem in vertical-illuminated APD [8]. With such package, the topmost metal contact in APD can serve as the reflector and enhance the photo-absorption process. However, as compared to the top-illuminated reference, the flip-chip bonded APD usually exhibits a less bandwidth due to the additional parasitic capacitance after package. Some alternative solutions, such as refracting facet [9] or installing a 45^{o} mirror, which is beneath the APD chip [6], have thus been demonstrated to fold the optical absorption path and eliminate the flip-chip bonding process. Nevertheless, the flip-chip bonding package integrated with a well fabricated substrate lens is still a very attractive solution due to that it offers the largest alignment tolerance and minimum size after co-package with low-loss free space optics among all the reported PD/APD packaging technologies [8]. In this work, we demonstrate a novel $In_{0.52}Al_{0.48}As$ backside-illuminated APDs with flip-chip bonding package and state-of-the-art performances. By optimizing the layouts for bonding process, such device can simultaneously exhibit superior bandwidth (36 vs. 31 GHz) and responsivity (3.4 vs. 2.3 A/W) than those of top-illuminated reference under 0.9 V_{br} operation and attain a high millimeter wave output power (-1 dBm at 40 GHz) and current (12.5 mA at +8.8 dBm optical power).

II. Device Structure

Figure 1 depicts the conceptual cross-sectional view of fabricated device structure. In order to release the trade-offs among speed, dark current, and responsivity, the dual M-layer structure is adopted [4,5]. By dividing the total M-layer thickness into two parts (1st and 2nd M-layer) with an additional charge control layer, a stepped electric field profile was introduced in the M-layer to attain high multiplication gain and smaller avalanche delay time. A composite charge layer ($In_{0.52}Al_{0.48}As$/InP) design is adopted to ensure that the electric field at the side wall of the bottom (2nd) M-layer becomes exactly zero and the phenomenon of edge breakdown is suppressed [10]. Here, three kinds of APDs were fabricated and investigated. Device A and B are APDs with two different layouts of AlN carriers for flip-chip bonding packages and C is the reference one with top-illuminated structure. All of them share the same epi-layer structure and same active window diameter as 14 μm, as shown in Figure 1. Figure 2 (a) to (d) shows the photos of metal pads on AlN carrier, top-view of devices B before flip-chip bonding and after flip-chip bonding, and device C respectively. Compared with device B, in device A, we have further optimized its layouts of metal pads on AlN carrier to improve the O-E bandwidth.

III.Measurement Result:

Figure 3(a) to (c) shows the measured bias-dependent dark current and photocurrent subjected to different optical pumping power at optical wavelength of 1.31 μm for devices (A to C). The measured breakdown voltage (V_{br}) is -26 V. Under low optical illumination power values (~10 μW) at 0.9 V_{br}, the measured responsivity is around 3.4, 3.1 and 2.3 A/W for the devices A to C, respectively. The gain versus bias voltages of our device under different optical pumping power (1 to1000 μW) are also provided in this figure for reference. As can be seen, the devices with flip-chip bonding package can have a higher responsivity (3.4 vs. 2.3 A/W) due to the fold of optical absorption path as expected. Moreover, under the same values of optical pumping power (-20 dBm), the maximum gain of device A is more than seven times larger (98 vs. 14 A/W [11]) than that of reported for its III-V [6] and Si-Ge [11] counterparts. This can be attributed to the lower dark current and more pronounced avalanche process facilitated by our dual M-layer design. Figures 4 and 5 shows the measured bias-dependent O-E frequency responses of all three devices under low (10 μW) and high (1 mW) optical pumping power at 1.55 μm wavelength, respectively. Compared with the reference device C, device B suffers the degradation in O-E bandwidth (27 vs. 30 GHz) under the same bias as 0.9 V_{br} due to the flip-chip bonding package induced parasitic capacitance as discussed. Nevertheless, device A with an optimized flip-chip bonding layout can have not only the highest responsivity (3.4 vs. 3.1 and 2.3 A/W) but also widest 3-dB bandwidths (36 vs. 27 and 30 GHz) among these three devices. Moreover, compared with the high-performance Si/Ge counterpart APDs with the same 14 μm window size [11], which is operated at around the same responsivity 3.5 (6.5) A/W, our demonstrated device A can have a superior 3-dB O-E bandwidth (36 (28) vs. 28 (22) GHz) [7]. On the other hand, under high (1 mW) optical power illuminations, these three devices (A to C) can maintain invariant 3-dB O-E bandwidths as 36, 27 and 30 GHz at 0.9 V_{br}, respectively. Such excellent high-power performance implies a good linearity and wide dynamic range of our demonstrated APDs. Figure 6 shows the photo-generated RF output saturation power measured with the heterodyne beating setup at a beating frequency of 40 GHz for device A and 30 GHz for devices B and C. All of them exhibit very close values of saturation current at 12 mA and maximum output RF power as -1 dBm under 0.9 V_{br}. This corresponds to a high launched optical power at +8.8 dBm for device A. Figure 7 shows the measured 3-dB bandwidths versus multiplication gain (M_G) of devices A to C. The values of gain-bandwidth product (GBP) under M_G=10 and extremely high gain of these three devices are all specified. We can clearly that with our optimized flip-chip bonding layout, we can have improvements in GBPs under high-sensivity operation (M_G=10) and with an unprecedented large maximum GBP up to 1 THz. Table 1 shows the benchmark of device A and the other reported high-speed APDs. Thanks to the novel dual M-layer design with an optimized flip-chip bonding package in device A, we can attain the lowest dark current, highest bandwidth-responsivity product, and largest overload and saturation optical power among these reported devices.

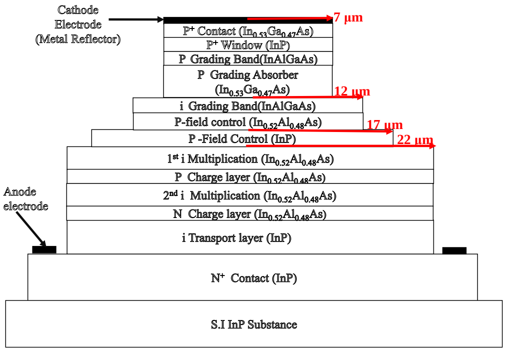

Figure 1. Conceptual cross-sectional views of the demonstrated.

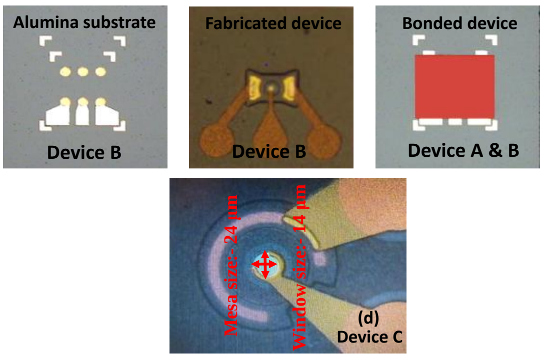

Figure 2. (a)-(d) The top-view of the fabricated Device B and C.

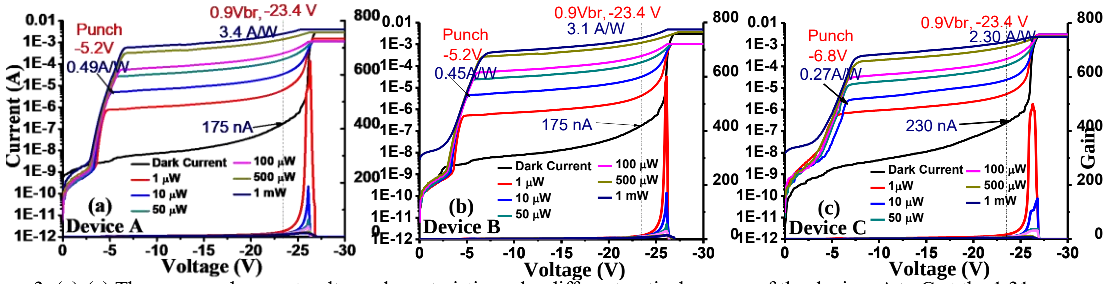

Figure 3. (a)-(c) The measured current voltage characteristic under different optical powers of the devices A to C at the 1.31 μm wavelength.

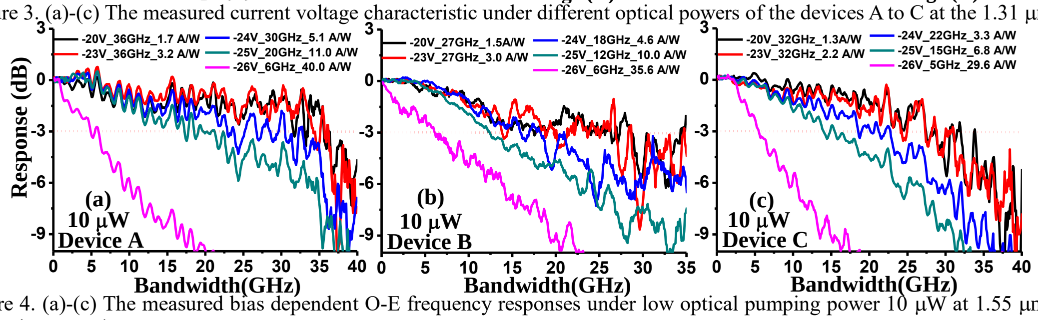

Figure 4. (a)-(c) The measured bias dependent O-E frequency responses under low optical pumping power 10 μW at 1.55 μm wavelength for devices A and C.

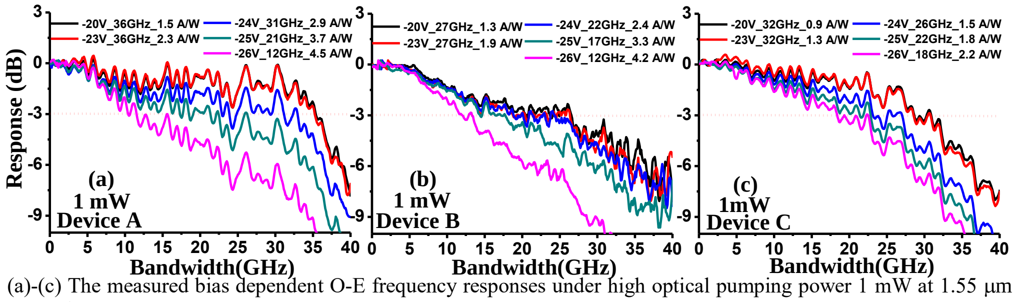

Figure 5. (a)-(c) The measured bias dependent O-E frequency responses under high optical pumping power 1 mW at 1.55 μm wavelength for devices A and C.

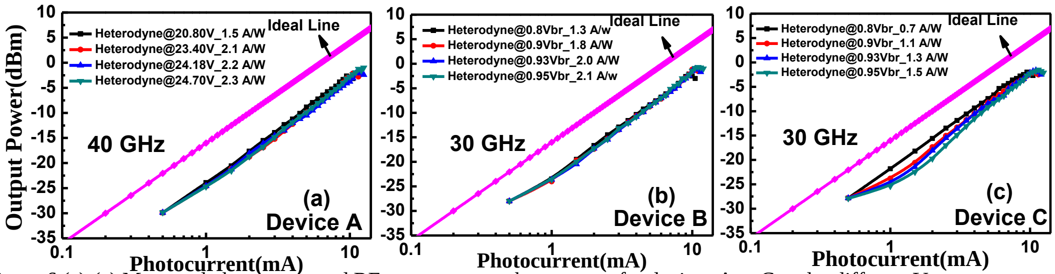

Figure 6 (a)-(c) Measured photo generated RF power versus photocurrent for devices A to C under different V_{br}.

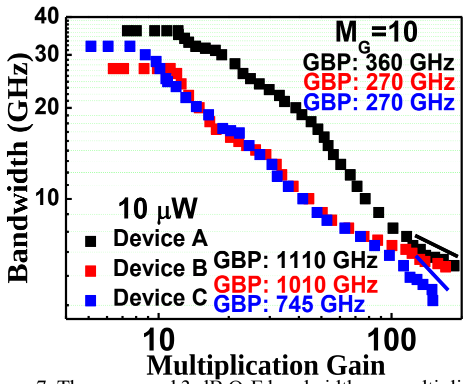

Figure 7. The measured 3-dB O-E bandwidths vs multiplication gain of APDs (A to C) at low (10 μW) optical pumping power.

Table 1 :- COMPARISON FOR DIFFERENT TYPES OF HIGH PERFORMANCE APDs

Parameter	NTT	SiFotonics technology	SEDI, JAPAN	This work
Reference	6	11	7	
Type	Backside illuminated	Topside-illuminated (Reflector on Backside)	Waveguide	Backside-illuminated
Window Size	14 μm	20 μm		14 μm
Dark Current (0.9 V_{br})	2 μA	0.9 μA	8μA	175 nA
Responsivity	1.95 A/W	3.53 (6.5) A/W	3.6 (9) A/W	3.4 (6.52) A/W
Bandwidth	28 GHz	28 (22) GHz	38(24) GHz	36 (28) GHz
Optical Saturation Power (Overload)	-6.3 dBm (Saturation)	< 0 dBm (Overload)	-	8.8 dBm (Saturation)

Summary:

In conclusion, by combing our dual M-layer design with our advanced flip-chip bonding package, we demonstrated a novel APD, which can simultaneously exhibit low dark current (175 nA), a wide 3-dB bandwidth at 36 GHz, high responsivity 3.4 A/W, high saturation current as 12 mA, and a high MMW output power (-1 dBm at 40 GHz) under the operation 0.9 V_{br}.

V. References:

[1] J. Cheng, C. Xie, Y. Chen, X. Chen, M. Tang and S. Fu, "Comparison of Coherent and IMDD Transceivers for Intra Datacenter Optical Interconnects," *Optical Fiber Communications Conference and Exhibition (OFC'2019)*, San Diego, CA, USA, Mar. 2019, W1F.2.

[2] M. Anagnosti, C. Caillaud, J.-F. Paret, F. Pommereau, G. Glastre, F. Blache, and M. Achouche, "Record Gain x Bandwidth (6.1 THz) Monolithically Integrated SOA-UTC Photoreceiver for 100-Gbit/s Applications," *J. Lightwave Technol.* vol., 33, no. 6, pp. 1186-1190, March 2015.

[3] T. Beckerwerth, R. Behrends, F. Ganzer, P. Runge and M. Schell, "Linearity Characteristics of Avalanche Photodiodes For InP Based PICs," *in IEEE Journal of Selected Topics in Quantum Electronics*, vol. 28, no. 2, pp. 1-8, March-April 2022, Art no. 3803408, doi: 10.1109/JSTQE.2021.3127853.

[4] Zohauddin Ahmad, Sheng-I Kuo, You-Chia Chang, Rui-Lin Chao, Naseem, Yi-Shan Lee, Yung-Jr Hung, Huang-Ming Chen, Jyehong Chen, Chee Seong Goh, and Jin-Wei Shi "Avalanche Photodiodes with Dual Multiplication Layers and Ultra-High Responsivity-Bandwidth Products for FMCW Lidar System Applications," *IEEE Journal of Selected Topics in Quantum Electronics*, vol. 28, no. 2, pp. 1-9, March-April 2022, Art no. 3800709, doi: 10.1109/JSTQE.2021.3062637.

[5] Naseem, P.-S. Wang, Z. Ahmad, S. H. Parvez, S. Yang, H.-S. Chen, H-S Chang, J. J.-S. Huang, and J.-W. Shi, "Top-illuminated Avalanche Photodiodes with Cascaded Multiplication Layers for High-Speed and Wide Dynamic Range Performance," *in Journal of Lightwave Technology*, 2022, doi: 10.1109/JLT.2022.3204743.

[6] M. Nada, Y. Yamada and H. Matsuzaki, "Responsivity-Bandwidth Limit of Avalanche Photodiodes: Toward Future Ethernet Systems," *IEEE Journal of Sel. Topics in Quantum Electronics*, vol. 24, no. 2, pp. 1-11, March-April 2018.

[7] T. Okimoto, K, Ashizawa, H. Mori, K. Ebihara, K. Yamazaki, S. Okamoto, K. Horino, Y. Ohkura, H. Yagi, M. Ekawa and Y. Yoneda " 106-Gb/s Waveguide AlInAs/GaInAs Avalanche Photodiode with Butt-joint Coupling Structure," *2022 Optical Fiber Communications Conference and Exhibition (OFC)*, 2022, pp. 01-03.

[8] Albis Optoelectronics AG, Moosstrasse 2a, 8803 Rueschlikon, Switzerland. (Product: APD20D1 on Submount).

[9] T. Takeshita, Y. Hirota, T. Ishibashi, Y. Muramoto, T. Ito, Y. Tohmori, and H. Ito, "Degradation behavior of avalanche photodiodes with a mesa structure observed using a digital OBIC monitor," *in IEEE Trans. on Electron Devices*, vol. 53, no. 7, pp. 1567-1574, July, 2006.

[10] Naseem, Z. Ahmad, Y.-M. Liao, P.-S. Wang, S. Yang, S.-Y. Wang, H.-S. Chang, H.-S. Chen, J. J.-S. Huang, E. Chou, Y.-H. Jan, and J.-W. Shi, "Avalanche Photodiodes with Composite Charge-Layers for Low Dark Current, High-Speed, and High-Power Performance," *IEEE Journal of Selected Topics in Quantum Electronics*, vol. 28, no. 2, pp. 1-10, March-April 2022.

[11] B. Shi, F. Qi, P. Cai, X. Chen, Z. He, Y. Duan, G. Hou, T. Su, S. Li, W. Chen, C. Hong, R.-Chen Yu and D. Pan., "106 Gb/s Normal-Incidence Ge/Si Avalanche Photodiode with High Sensitivity," *2020 Optical Fiber Communications Conference and Exhibition (OFC)*, 2020, pp. 1-3.